Article

Discovery Medicine 2025; 37(194): 573–582
https://doi.org/10.24976/Discov.Med.202537194.49

The Correlation between GSK3β and miR-140 and its Effect on the Pathogenesis of Asthma

Ting Yang[1], Chang Xu[1], Niu Ding[1], Shujuan Luo[1], Liyan Luo[1], Shijie Jin[1], Yanping Chen[1,*]

[1]Department of Respiratory Medicine, Hunan Children's Hospital, 410000 Changsha, Hunan, China
*Correspondence: yanpingchenmrs@sina.com (Yanping Chen)
Published: 20 March 2025

Background: MicroRNAs (miRNAs) are linked to asthma progression. In this study, we aimed to decipher the functional role of miR-140 and delineate its link to the mechanism behind the progression of asthma.
Methods: BALB/c mice were divided into four groups, designated as control, asthma, Agomir negative control (NC), and Agomir group. *In vitro* model of asthma using transforming growth factor-beta 1 (TGF-β1)-treated 16HBE cells, and cells transfected with glycogen synthase kinase 3β (GSK3β) overexpression plasmid or Agomir miR-140. Real-time quantitative polymerase chain reaction (RT-qPCR) was to test miR-140 abundance. Hematoxylin and eosin (HE) and periodic acid-Schiff (PAS) of lung tissues for examining their histopathological changes. Enzyme-linked immunosorbent assay (ELISA) and *in situ* terminal deoxynucleotidyl transferase dUTP nick end labeling (TUNEL) were to test inflammatory factors levels and cell apoptosis, respectively. B-cell lymphoma 2 (Bcl-2), GSK3β, cleaved caspase-3 and Bcl-2 associated X protein (BAX) protein levels were evaluated using Western blotting. GSK3β expression was also detected using immunohistochemistry (IHC). RNA immunoprecipitation (RIP) and dual-luciferase reporter assay were to verify the correlation between GSK3β and miR-140.
Results: Both the asthma mice and TGF-β1-treated 16HBE cells exhibited decreased miR-140 level and increased protein expression of GSK3β ($p < 0.001$). Compared with the asthma mice, overexpression of miR-140 significantly relieved airway inflammation and reduced cell apoptosis ($p < 0.001$). Targeted relationship existed between GSK3β and miR-140, and the overexpression of miR-140 dramatically repressed the level of GSK3β in asthma group and TGF-β1-treated 16HBE cells ($p < 0.001$). Nevertheless, the suppressive impacts of miR-140 overexpression were hindered by GSK3β upregulation in TGF-β1-treated 16HBE cells ($p < 0.01$ or $p < 0.001$).
Conclusions: miR-140 mitigates airway inflammation and represses apoptosis in asthma by targeting and regulating GSK3β.

Keywords: asthma; miR-140; airway inflammation; GSK3β

Introduction

Asthma belongs to the chronic inflammatory disease, recognized by airway inflammation, airflow obstruction, and bronchospasms [1–3]. While a host of factors such as infection, smoking, and allergens are reportedly the inducers of asthma [4,5], the molecular pathogenesis of asthma remains largely unknown. Therefore, the identification of valid biomarkers that can predict asthma progression is of great significance in the planning of treatments.

A growing researches substantiated the critical role of miRNAs in the progression of asthma [6,7]. For instance, miR-203a-3p regulates the Smad3 pathway in asthma by targeting Sine oculis homeobox homolog 1 (*SIX1*) [8]; miR-451a targets cadherin 11 to suppress airway remodeling in asthma [9]; and miR-135b regulates chemokine C-X-C motif ligand 12 (CXCL12) to inhibit asthma-associated airway inflammation [10]. miR-140, a micro-Ribonucleic Acid (miRNA) family member, has been widely demonstrated the major functions in a wide range of diseases. For instance, miR-140/Sphingosine-1-phosphate receptor 1 (S1PR1) axis has been found to relieve neuropathic pain in chronic constriction injury rats [11]. Nevertheless, miR-140 is not always playing a role beneficial to health; in fact, miR-140-3p has been found to target phosphatase and tensin homolog (*PTEN*), leading to the deterioration of osteoporosis through the PTEN/phosphoinositide 3-kinase (PI3K)/threonine kinase (AKT) pathway [12]. In the realm of pulmonary diseases, the expression of miR-140-3p has been found to be low in asthma [13]. Meng *et al*. [14] reported the decline of miR-140-3p in the plasma of asthmatic patients, and reported the inhibitory utility of miR-140-3p on JAK/STAT3 signaling by targeting high mobility group box 1 (HMGB1), and the ameliorative effect on airway inflammation. Although these studies have demonstrated the effects of miR-140 in asthma [13–15], the underlying mechanisms still need to be discovered.

Glycogen synthase kinase 3 (GSK3), a serine-threonine kinase, has pathological links to an array of diseases [16,17]. The chief function of GSK3 is to regulate a variety of cellular functions, such as differen-

tiation, metabolism, immune activation, apoptosis, and survival [18]. GSK3 manifests in two forms—GSK3α and GSK3β—with the latter playing a modulatory role in airway inflammation, based on a study on asthmatic mice [19]. It has been found that melatonin regulated the signal transducer and activator of transcription 3 (STAT3)/AKT/GSK3β to alter the phenotype of airway smooth muscle cells, thereby demonstrating improved efficacy in asthma [20]. The effects of miR-140 on GSK3β were probed, for instance, miR-140-5p could regulate the GSK3β to mediate iron death in hemoglobin-induced neurons [21]. In sepsis mice, miR-140 up-regulation exhibited an inhibitory effect on GSK3β [22]. But it is uncertain whether miR-140 is involved in the pathogenesis of asthma by regulating GSK3β.

Interleukin (IL)-5 and IL-13 are mainly released by T helper 2 cells, have the capacity to regulate the proliferation and differentiation of B cells and eosinophils, and the elevated IL-5 and IL-13 expression levels were found in lung tissues of asthmatic mice [19,23]. Transforming growth factor beta 1 (TGF-β1) is an important regulatory factor in immunity, plays a complex and intertwined role in inflammation, T cell differentiation, and immune suppression [24]. These inflammatory mediators are closely related to the pathology of asthma [25]. In our study, the purpose was to investigate the role of miR-140 on asthma progression, and explore the potential mechanisms. We established *in vivo* and *in vitro* asthmatic models to evaluate the changes and influence miR-140 expression. Moreover, the correlation between GSK3β and miR-140 was also evaluated to decipher the mechanism underlying the development of asthma linked to miR-140.

Materials and Methods

Animal Experiments

This study was approved by the Committee on Animal Experimentation of Hunan Children's Hospital and performed in compliance with the Guidelines for the Care and Use of Laboratory Animals (No.2020040301).

A total of 24 male BALB/c mice (18–20 g; 4 to 6 weeks old) acquired from Vital River Co. Ltd. (Beijing, China) were maintained in a regular day/night cycle room, temperature set at 22–25 °C. Water and food were supplied in sufficient quantities and freely available. All mice were adaptively fed for 7 days. Four groups were established (n = 6 for each group): control, asthma, Agomir negative control (NC), and Agomir group.

To establish an asthmatic mice model, the mice were intraperitoneally injected with $Al(OH)_3$ (20 mg; 1017502, Sigma-Aldrich, St. Louis, MO, USA) and ovalbumin (OVA; 20 µg; A5503, Sigma-Aldrich, St. Louis, MO, USA) in 200 µL phosphate-buffered saline (PBS) on day 0 and day 14 for sensitization. Then, 1% aerosolized OVA/PBS was used to treat the mice using an ultrasonic nebulizer (402AI, Jiangsu Yuyue Medical Equipment and Supply Co., Ltd., Jiangsu, China) on days 27–30; the treatment was administered once per day. The mice of the control group were treated with 200 µL of PBS. The mice were treated with Agomir miR-140 (25 mg/kg/day; B06001, GenePharma, Shanghai, China) in the Agomir group, whereas those in the Agomir NC group were treated with negative control (25 mg/kg/day; B04008, GenePharma, Shanghai, China) through tail vein injection from days 27 to 30. Eventually, all mice were euthanized through cervical dislocation.

Cell Culture

16HBE cells (FY-22FN1403; human bronchial epithelial cell line) were obtained from the Shanghai Fuyu Biotechnology Co., Ltd. (Shanghai, China). Short tandem repeat (STR) certification and mycoplasma testing had been performed prior to utilization. All cells were cultured in Dulbecco's Modified Eagle Medium (DMEM; Gibco, Carlsbad, CA, USA) supplemented with 10% fetal bovine serum (30067334, Thermo Fisher Scientific, Waltham, MA, USA), and placed at an incubator (37 °C, 5% CO_2 ambiance).

Six-well plates were for the 24 h cultivation of 16HBE cells (2×10^5 cells/well, cells suspended in 2 mL culture medium in each well). To up-regulate miR-140, 50 nM of Agomir miR-140 was transfected into 16HBE cells using Lipofectamine® 2000 (11668027, Invitrogen, Carlsbad, CA, USA) for 48 h. Agomir NC was used as a negative control. GSK3β overexpression plasmid (GSK3β) and the empty pcDNA3.1 vector (GSK3β NC) were transfected into 16HBE cells according to the operation instructions for Lipofectamine® 2000 (11668027, Invitrogen, Carlsbad, CA, USA).

Cell Model

TGF-β1 was acquired from Absin (abs44075406; Absin Bioscience Inc., Shanghai, China) and dissolved in 10 mM citric acid, the solution was stored at –20 °C. 16HBE cells cultured in 6-well plates (2×10^5 cells/well) were treated with TGF-β1 (10 ng/mL) to establish an asthma cell model *in vitro* and then harvested for further investigations.

Bronchoalveolar Lavage Fluid Collection

After sacrificing the mice, their lungs were perfused with PBS and a catheter was inserted into the trachea. PBS (3 mL) was infused into the lung to obtain bronchoalveolar lavage fluid (BALF). The cells in a fresh BALF sample were enumerated using a hemocytometer. The slides were prepared with cytospin (Cytospin 3, Thermo Shandon, Runcorn, UK) and Diff-Quik (Baxter Healthcare Corp, Deerfield, IL, USA) for staining. Cell types were evaluated under a light microscope, with at least 500 cells per slide.

Real-Time Quantitative Polymerase Chain Reaction (RT-qPCR)

Total RNA extracted from the 16HBE cells or lung tissues was isolated with TRIzol reagent (15596018, Invitrogen, Carlsbad, CA, USA). A miRNA First-Stand cDNA Synthesis Kit (K1621, GeneCopoeia, Rockville, MD, USA) was used to generate cDNA. SYBR Green PCR kit (420A, TaKaRa, Dalian, China) was employed for PCR run on the Applied Biosystems 7500 Real-time PCR Systems (Thermo Fisher Scientific, Foster, CA, USA). The relative expression of miR-140 was calculated using the $2^{-\Delta\Delta Ct}$ method and normalized to the expression of *U6*. The sequences of primers are presented in Table 1.

Table 1. Primer sequences for RT-qPCR.

Gene	Sequences (5′-3′)
miR-140	Forward: GAGTGTCAGTGGTTTTACCCT
	Reverse: GCAGGGTCCGAGGTATTC
U6	Forward: CTCGCTTCGGCAGCACA
	Reverse: AACGCTTCACGAATTTGCGT

RT-qPCR, real-time quantitative polymerase chain reaction.

Histopathological Examination of the Lung Tissues

The lung tissues obtained from mice were fixed in 4% neutral formaldehyde, embedded in paraffin, made into 4 µm sections, and stained with hematoxylin and eosin (HE). Finally, the sections were observed under an optical microscope (BX41; Olympus, Tokyo, Japan). The inflammation score in HE staining results was evaluated in blindway referring to previous studies [26,27]. The scoring criteria were set as grade 0 (no inflammatory cells), grade 1 (occasional/few inflammatory cells), grade 2 (alveolar wall thickening, increased macrophages and eosinophils in alveolar), grade 3 (alveolar walls significantly thickened, multinucleated giant cells and eosinophils in 30–50% of alveoli), grade 4 (alveolar walls significantly thickened, multinucleated giant cells and eosinophils in more than 50% of alveoli), grade 5 (alveolar consolidation).

In parallel, the tissue specimens were also stained with periodic acid-Schiff (PAS; Baso Diagnostic, Zhuhai, China) to assess changes in the morphology of goblet cells and the level of mucus secretion. A quantitative analysis was conducted to measure the PAS-positive area. The five airway sections randomly distributed throughout the left lung were examined and the scores were calculated.

Enzyme-Linked Immunosorbent Assay (ELISA)

The level of TGF-β1, IL-5, and IL-13 levels in the serum, BALF and cell supernatant were determined using the corresponding ELISA kit following the operating protocols. The TGF-β1 (EK981), IL-5 (EK205), and IL-13 (EK213) ELISA kits were purchased from MultiSciences (Hangzhou, China).

Immunohistochemistry

After deparaffinization, the specimens were rehydrated in a graded ethanol series, and microwaved for antigen retrieval. Subsequently, primary antibody anti-GSK3β (1:500; ab32391, Abcam, Cambridge, UK) was used for specimen incubation overnight at 4 °C. Then, specimens were incubated with the secondary antibody (1:2000; ab205718, Abcam, Cambridge, UK). The specimens were stained with diaminobenzidine (DAB) followed by counterstaining with hematoxylin. Finally, the specimens were photographed using a microscope (Ti2-U; ECLIPSE, Nikon, Tokyo, Japan).

Western Blotting

The total proteins in lung tissues or 16HBE cells were extracted using RIPA reagent (P0013B, Beyotime, Shanghai, China). Proteins (30 µg) were loaded onto a 12% sodium dodecyl sulphate-polyacrylamide gel electrophoresis (SDS-PAGE; 161-1176, Bio-Rad, San Jose, CA, USA) for separation. Then, the protein bands were transferred from the gel to the polyvinylidene difluoride (PVDF) membranes (1620177, Bio-Rad, San Jose, CA, USA). After incubation with 5% non-fat milk for 1.5 h, the membranes were then treated with anti-B-cell lymphoma-2 (Bcl-2) associated X protein (BAX) (1:1000; ab32503, Abcam, Cambridge, UK), anti-GSK3β (1:5000; ab32391, Abcam, Cambridge, UK), anti-cleaved caspase-3 (1:1000; ab32042, Abcam), anti-β-actin (1:1000; ab8227, Abcam, Cambridge, UK), and anti-Bcl-2 (1:1000; ab182858, Abcam, Cambridge, UK) overnight at 4 °C, followed by incubation with the goat anti-rabbit IgG H&L antibody (HRP) (1:10,000, ab205718, Abcam, Cambridge, UK) at room temperature for 2 h. Protein bands were evaluated using an enhanced chemiluminescence (ECL) kit (35055, Pierce, Thermo Fisher Scientific, Waltham, MA, USA). Signal intensity was quantified using ImageJ (Ver. 1.52b; NIH, Bethesda, MD, USA) and the target protein signal in each lane was normalized by the signal value of the internal loading control.

TUNEL Staining

The lung tissue specimens were dipped into a Triton X-100 solution (0.2%) and incubated with the terminal deoxynucleotidyl transferase dUTP nick end labeling (TUNEL) reaction mixture (50 µL; 11684817910, Roche Applied Science, Mannheim, Germany) and 3,3′-diaminobenzidine (DAB, 50 µL). Microscope (Ti2-U; ECLIPSE, Nikon, Tokyo, Japan) was used for observation and photography.

The treated 16HBE cells were stained with the TUNEL reaction mixture (50 µL, 11684795910, Roche, Mannheim, Germany) and counterstained with 4′,6-diamidino-2-phenylindole (DAPI) (10236276001, Sigma-Aldrich, St. Louis, MO, USA). Finally, the TUNEL-positive cells were imaged using a microscope (FV1000, Olympus, Tokyo, Japan).

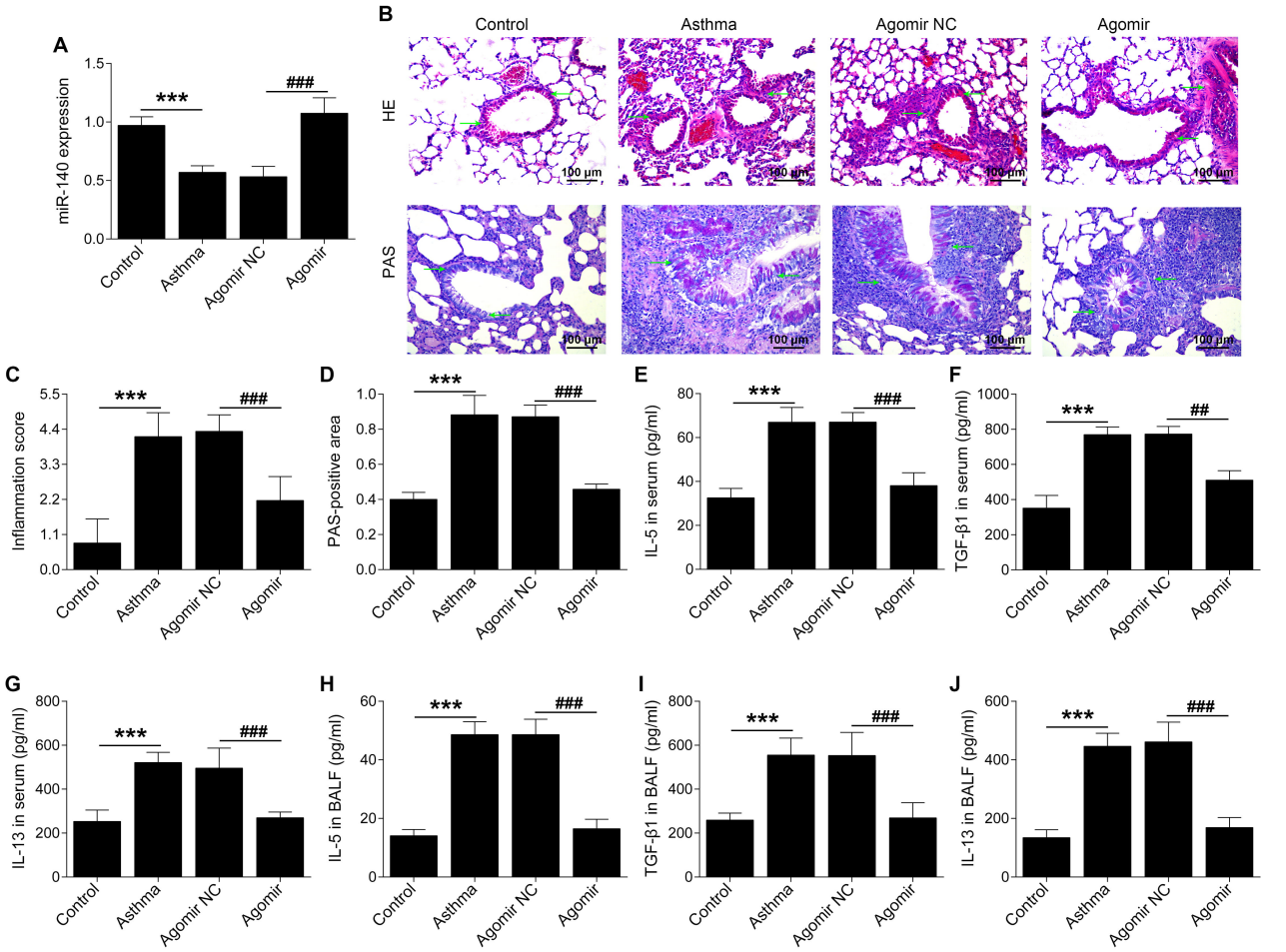

Fig. 1. miR-140 attenuates airway inflammation in asthmatic mice. (A) miR-140 expression in lung tissue from the mice was examined using RT-qPCR. (B) The lung histopathological changes were confirmed with hematoxylin and eosin (HE) and periodic acid-Schiff (PAS) staining (scale bar: 100 μm). Green arrows indicated the inflammatory infiltration. (C) The inflammation score based on HE staining was determined. (D) The PAS-positive area was analyzed. (E–G) Interleukin (IL)-5, transforming growth factor beta 1 (TGF-β1), and IL-13 levels in the serum were determined with enzyme-linked immunosorbent assay (ELISA). (H–J) IL-5, TGF-β1, and IL-13 levels in the bronchoalveolar lavage fluid (BALF) were determined with ELISA. n = 6; ***$p < 0.001$ versus control group; $^{\#\#}p < 0.01$, $^{\#\#\#}p < 0.001$ versus Agomir NC group. NC, negative control.

Dual-luciferase Reporter Assay

Targetscan 6.0 online database (http://www.targetscan.org) was applied to predict the sequences of binding sites of miR-140 on *GSK3*β. The wild-type reporter *GSK3*β- wild-type (WT) (containing the binding sites of miR-140) and the mutant-type reporter *GSK3*β- mutant-type (MUT) (mutation in the binding sites) were constructed. The Agomir NC and Agomir miR-140 were co-transfected with GSK3β-WT and GSK3β-MUT into 16HBE cells following the manual of Lipofectamine® 2000 (Invitrogen, Carlsbad, CA, USA). Dual-luciferase reporter assay system (E1960, Promega, Madison, WI, USA) was applied to test the luciferase activity.

RNA Immunoprecipitation (RIP) Assay

The harvested cell supernatants were incubated with Ago2 (1:1000; MABE253, EMD Millipore, Billerica, MA, USA) or mouse IgG (1:2000; SAB5600195, EMD Millipore, Billerica, MA, USA) overnight at 4 °C and cultured with protein A/G magnetic beads (4 h, 4 °C). The immunoprecipitated RNA was measured using RT-qPCR.

Statistical Analysis

The raw experimental data was analyzed using SPSS 20.0 (SPSS, Inc., Chicago, IL, USA). The data are expressed as mean $\pm$ standard deviation (SD). The difference among multiple groups was compared using one-way analysis of variance (ANOVA) and post hoc Bonferroni test. Difference with $p < 0.05$ was considered statistically significant.

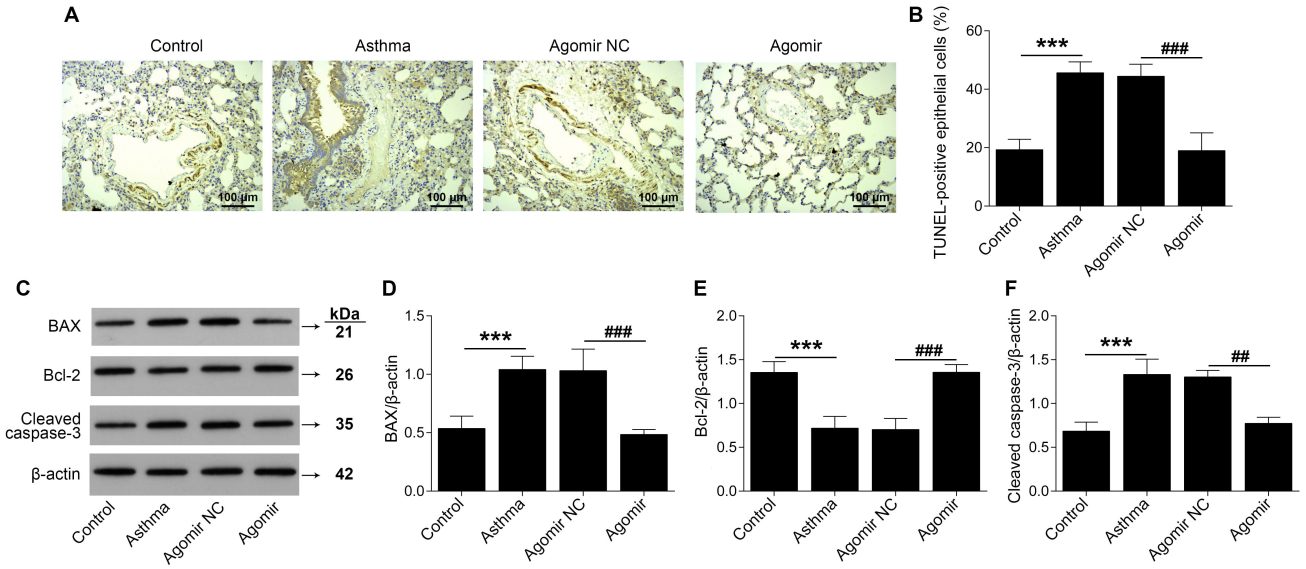

Fig. 2. miR-140 inhibits apoptosis in lung tissues of asthmatic mice. (A,B) Apoptosis cells in the lung tissues were evaluated using terminal deoxynucleotidyl transferase dUTP nick end labeling (TUNEL) assay (scale bar: 100 μm). (C–F) Western blotting for assessing the protein levels of cleaved caspase-3, B-cell lymphoma-2 (Bcl-2), and Bcl-2 associated X protein (BAX). n = 6; ***$p < 0.001$ versus control group; $^{\#\#}p < 0.05$, $^{\#\#\#}p < 0.001$ versus Agomir NC group.

Results

miR-140 Attenuates Airway Inflammation in Asthmatic Mice

The level of miR-140 expression was dramatically downregulated in the asthma group ($p < 0.001$), and upregulated following the overexpression of miR-140 in lung tissue homogenates ($p < 0.001$) (Fig. 1A). HE and PAS staining showed that there was a surge in inflammatory infiltration into the vessels, bronchus, and pulmonary mesenchyme in the lung tissues of the asthma mice, but this inflammatory phenomenon was downplayed after miR-140 overexpression (Fig. 1B). Additionally, the inflammation score and the PAS-positive area were also increased in the asthma group ($p < 0.001$), but could be reversed following miR-140 upregulation ($p < 0.001$) (Fig. 1C,D). The ELISA results revealed that IL-5, TGF-β1, and IL-13 levels in the serum and BALF were elevated in the asthma group ($p < 0.001$); however, this effect was relieved following miR-140 overexpression ($p < 0.01$ or $p < 0.001$) (Fig. 1E–J).

miR-140 Inhibits Apoptosis in Lung Tissues of Asthmatic Mice

As shown in Fig. 2A,B, the apoptosis happened to a greater extent in the asthma group ($p < 0.001$), but the Agomir miR-140 could inhibit this cellular event in the lung tissues of asthma mice ($p < 0.001$). In the asthma group, the BAX and cleaved caspase-3 protein levels were significantly upregulated ($p < 0.001$), whereas anti apoptotic protein Bcl-2 was markedly downregulated ($p < 0.001$); however, miR-140 overexpression could reverse these effects ($p < 0.01$ or $p < 0.001$) (Fig. 2C–F).

miR-140 Suppresses GSK3β Expression in Asthmatic Mice

Immunohistochemical analysis revealed the increased GSK3β expression level in the lung tissues in the asthma group ($p < 0.001$), which was however attenuated by the upregulation of miR-140 ($p < 0.001$) (Fig. 3A,B). GSK3β protein expression was obviously augmented in asthmatic mice ($p < 0.001$), and this effect could be suppressed by overexpressing miR-140 ($p < 0.001$) (Fig. 3C,D). Taken together, miR-140 suppressed GSK3β expression in asthmatic mice.

GSK3β is a Target of miR-140

Targeted binding sequence of miR-140 and *GSK3β*, retrieved from Targetscan website, are shown in Fig. 4A. miR-140 overexpression lowered the luciferase activity of the GSK3β-WT vectors ($p < 0.001$), whereas did not impact the luciferase activity of the GSK3β-MUT ($p > 0.05$) (Fig. 4B). GSK3β and miR-140 were preferentially enriched in the Ago2-containing micro-ribonucleoproteins in the 16HBE cells ($p < 0.001$) (Fig. 4C). 16HBE cells were induced by TGF-β1 to establish an asthma cell model. The level of miR-140 expression was reduced after TGF-β1 stimulation and enhanced following the overexpression of miR-140 ($p < 0.001$) (Fig. 4D). GSK3β protein level was upregulated in the asthmatic cell model ($p < 0.001$), which was partially blocked by miR-140 overexpression ($p < 0.001$) (Fig. 4E,F).

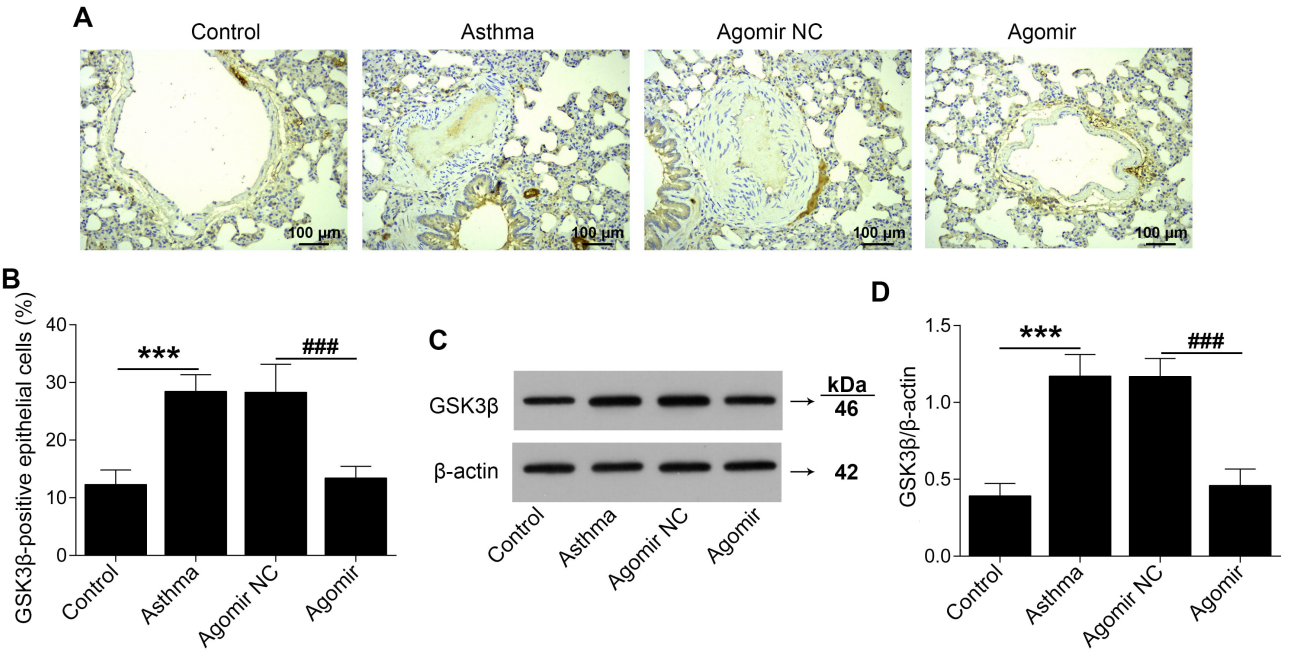

Fig. 3. miR-140 suppresses glycogen synthase kinase 3β (GSK3β) expression in asthmatic mice. (A,B) The GSK3β expression in lung tissues was confirmed through immunohistochemistry (IHC) in lung tissues (scale bar: 100 μm). (C,D) The protein expression level of GSK3β was examined by means of Western blotting. n = 6; ***$p < 0.001$ versus control group; $^{###}p < 0.001$ versus Agomir NC group.

GSK3β Upregulation Attenuates the Impacts of miR-140 on Inflammation and Apoptosis in Asthma

Rescue assays were performed in TGF-β1-induced 16HBE cells to confirm whether GSK3β is associated with the effect. The levels of TGF-β1, IL-5 and IL-13 were upregulated in the 16HBE cells ($p < 0.001$) and reduced after miR-140 was overexpressed ($p < 0.001$); nevertheless, the protective effect of miR-140 upregulation could be reversed by overexpressing GSK3β ($p < 0.01$ or $p < 0.001$) (Fig. 5A–C). The apoptosis rate of 16HBE cells was overtly increased ($p < 0.01$). Although the upregulation of miR-140 could reduce the level of apoptosis ($p < 0.01$), we found that the GSK3β overexpression could restore the apoptosis rate ($p < 0.01$) (Fig. 5D,E). In addition, TGF-β1 enhanced the pro-apoptotic protein levels, including BAX and cleaved caspase-3 ($p < 0.001$), while the Bcl-2 protein level was markedly lowered in 16HBE cells ($p < 0.001$). GSK3β overexpression inhibited the impacts of miR-140 upregulation on the expression of BAX, Bcl-2 and cleaved caspase-3 ($p < 0.01$ or $p < 0.001$) (Fig. 5F–I). Taken together, GSK3β overexpression weakened the beneficial impacts of miR-140 on inflammation and apoptosis, which are associated with asthma.

Discussion

The principal findings of the current study are the significantly decreased expression of miR-140 in asthmatic mice, and the improvement in asthma-related inflammation and suppression in apoptosis mediated by miR-140 upregulation. We also found that the expression of GSK3β was increased in asthmatic mice. In addition, rescue experiments uncovered that the attenuation of inflammation and apoptosis mediated by miR-140 upregulation could be blocked by GSK3β elevation in 16HBE cells.

A growing line of evidence has corroborated the vital and multifaceted roles of miRNAs in asthma [28,29]. Previous studies have already demonstrated that miR-140-3p is abnormally expressed in asthma [13,14]. The findings in this study stretched our understanding further, revealing that miR-140 was downregulated in asthmatic mice and TGF-β1-treated 16HBE cells. The changes in miR-140 were consistent with the trends of miR-140-3P previously reported in asthma [13]. Next, the protective effect of miR-140 was confirmed by a series of experiments involving the overexpression of miR-140, marked by its ability to alleviate the asthma-mediated inflammatory infiltration into the vessels, bronchus, and pulmonary mesenchyme in the lung tissues, a pathological condition known to be triggered by inflammatory reactions in asthma [30,31]. The inflammatory cells contribute to the deterioration of asthma and accelerated progression by facilitating the generation and release of IL-5, IL-13, tumor necrosis factor alpha (TNF-α), TGF-β1 and IL-1β, which collectively promote airway inflammation [32–34]. Therefore, reducing inflammation was an important treatment goal for asthma. The influences of miR-140 on inflammatory factors were also found. For example, miR-140 diminished the secretion of inflamma-

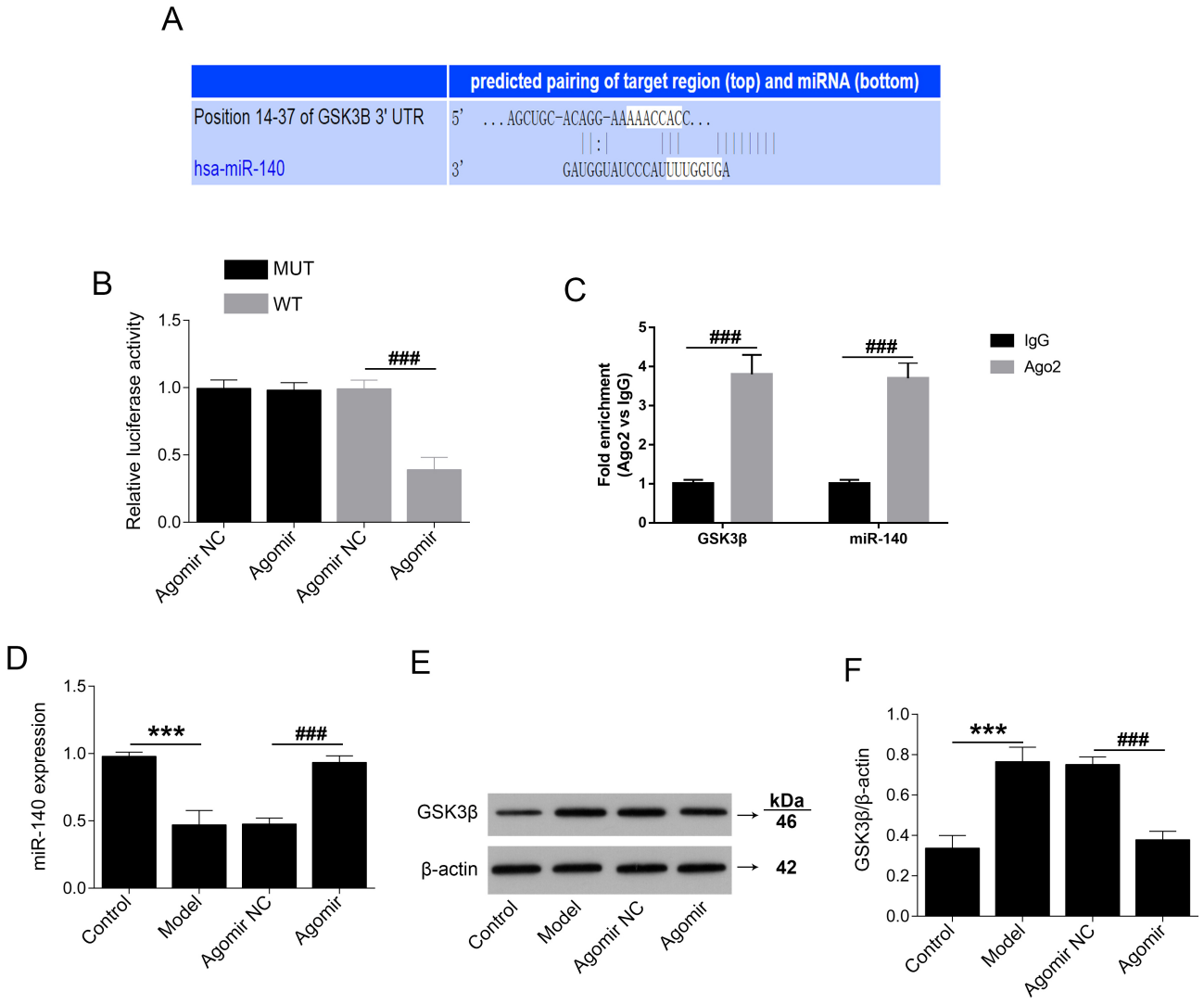

Fig. 4. GSK3β is a target of miR-140. (A) The binding sites of miR-140 on *GSK3β* were predicted through the Targetscan website. (B) Dual-luciferase reporter assay was to verify the targeting relationship between GSK3β and miR-140. (C) The interaction between miR-140 and GSK3β was determined by RNA immunoprecipitation (RIP) assays. (D) The expression level of miR-140 was assessed by means of RT-qPCR. (E,F) The protein expression level of GSK3β was examined using Western blotting. n = 3; $^{***}p < 0.001$ versus control group; $^{\#\#\#}p < 0.001$ versus Agomir NC group.

tory factors in the dorsal root ganglions of chronic constriction injury [11], and its mitigation effect on IL-1β and TNF-α was found in the myocardial ischemia-reperfusion injury model mice [35]. In this study, we discovered that miR-140 upregulation could reduce the levels of TGF-β1, IL-5 and IL-13, which were otherwise elevated in the asthmatic milieu, as tested in animal and cellular models. These results suggested that miR-140 could alleviate airway inflammation in asthma. The impacts of miR-140 on inflammatory factors were consistent with previous literature. Apart from that, we found that miR-140 upregulation lent itself to the inhibition of bronchial epithelial cell apoptosis in asthmatic mice and TGF-β1-treated 16HBE cells.

GSK3β could acts as a potent driver of inflammation [36,37]. GSK3β specific inhibitor reduced the TNF-α level in *Porphyromonas gingivalis* lipopolysaccharide-affected microglia cells [38]. The negative regulatory relationships between GSK3β and miR-140 were found in a previous study [21]. Our study validated the targeting relationship between miR-140 and GSK3β by dual fluorescein assay and RIP assay. It also showed that miR-140 downregulated GSK3β, provides protection against inflammation and apoptosis in asthma mice and TGF-β1-treated 16HBE cells. Moreover, the improvement in inflammation and apoptosis brought about by miR-140 upregulation could be reversed by GSK3β overexpression in TGF-β1-treated 16HBE cells. These results proved that miR-140 negatively regulated GSK3β and thus reduced inflammatory responses, consistent with previous study.

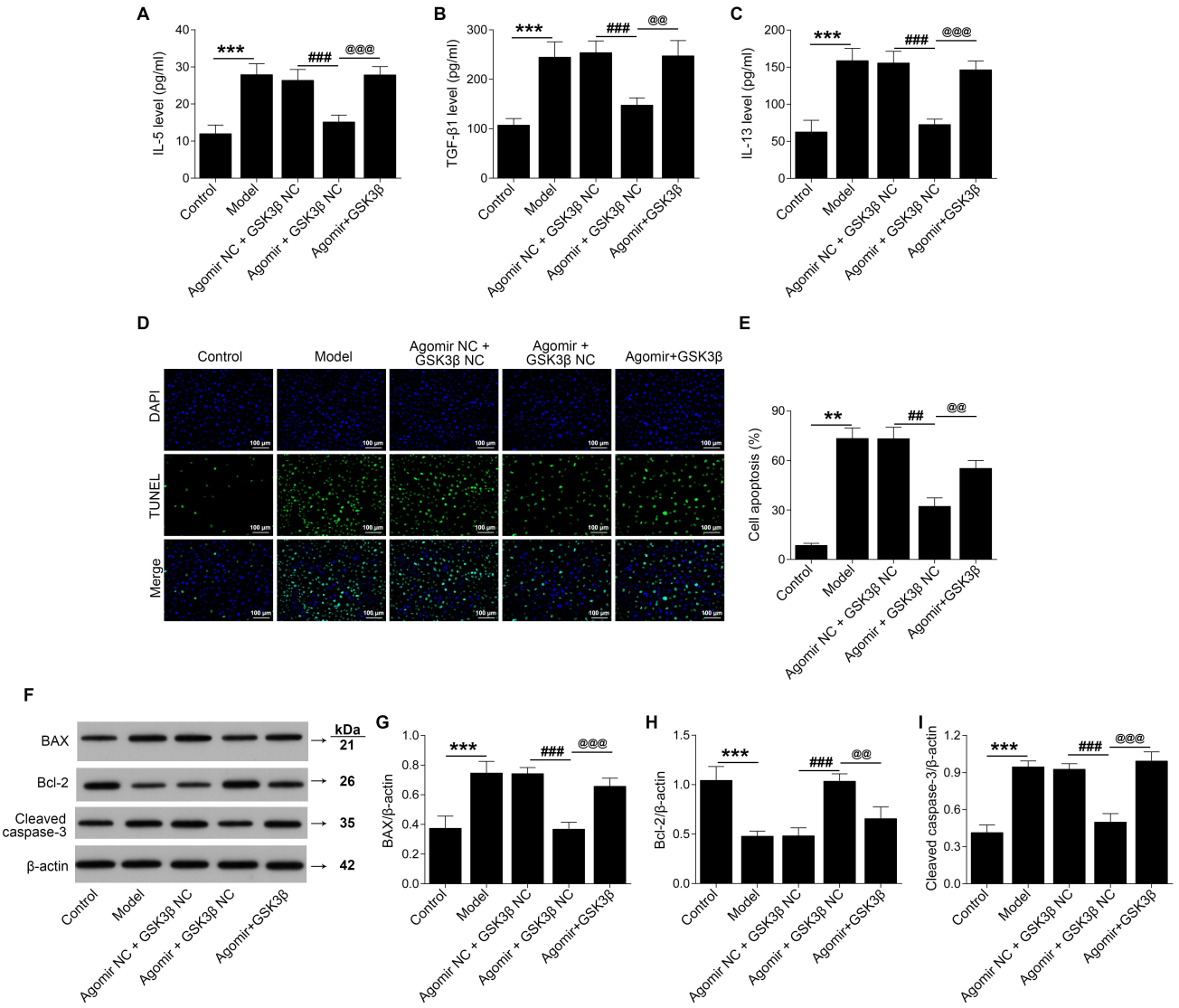

Fig. 5. GSK3β upregulation weakens the impacts of miR-140 on inflammation and apoptosis in 16HBE cells. (A–C) IL-5, TGF-β1 and IL-13 levels in 16HBE cells were measured using ELISA. (D,E) TUNEL assay was conducted to assess apoptosis (scale bar: 100 µm). (F–I) Protein levels of BAX, Bcl-2 and cleaved caspase-3 were assessed by means of Western blotting. n = 3; $^{**}p < 0.01$, $^{***}p < 0.001$ versus control group; $^{\#\#}p < 0.01$, $^{\#\#\#}p < 0.001$ versus Agomir NC + GSK3β NC group; $^{@@}p < 0.01$, $^{@@@}p < 0.001$ versus Agomir + GSK3β NC group. DAPI, 4′,6-diamidino-2-phenylindole.

There were some limitations in this study. Firstly, we did not evaluate the impacts of GSK3β alone on inflammation and apoptosis in asthmatic mice and TGF-β1-treated 16HBE cells. Secondly, we did not perform the rescue experiments *in vivo*. These limitations serve as reference points in future experiments. In conclusion, the current study elucidates the role of miR-140 in asthma and the implication of GSK3β therein, which may provide new insights into the pathomechanisms of asthma and a basis for therapeutic target development.

Conclusions

In summary, asthmatic mice and cellular models exhibit reduced levels of miR-140 and increased levels of GSK3β. In the same vein, miR-140 serves as a protective factor in asthma for suppressing inflammation and apoptosis, which can however be reversed by the overexpression of GSK3β, a target of miR-140.

Availability of Data and Materials

All data included in this study are available upon request by contact with the corresponding author.

Author Contributions

TY, CX and YPC designed the research study and wrote first draft. TY and ND performed the research. SJL and LYL provided help and advice on the ELISA experiments. SJJ analyzed the data. All authors contributed significantly to editorial changes of important content. All authors read and approved the final manuscript. All authors have participated sufficiently in the work and agreed to be accountable for all aspects of the work.

Ethics Approval and Consent to Participate

All animal experiments were approved by the Committee on Animal Experimentation of Hunan Children's Hospital and performed in compliance with the Guidelines for the Care and Use of Laboratory Animals (No.2020040301).

Acknowledgment

Not applicable.

Funding

This research received no external funding.

Conflict of Interest

The authors declare no conflict of interest.

References

[1] Varricchi G, Ferri S, Pepys J, Poto R, Spadaro G, Nappi E, *et al*. Biologics and airway remodeling in severe asthma. Allergy. 2022; 77: 3538–3552.

[2] Kuruvilla ME, Lee FEH, Lee GB. Understanding Asthma Phenotypes, Endotypes, and Mechanisms of Disease. Clinical Reviews in Allergy & Immunology. 2019; 56: 219–233.

[3] Peters U, Dixon AE, Forno E. Obesity and asthma. The Journal of Allergy and Clinical Immunology. 2018; 141: 1169–1179.

[4] Barnthouse M, Jones BL. The Impact of Environmental Chronic and Toxic Stress on Asthma. Clinical Reviews in Allergy & Immunology. 2019; 57: 427–438.

[5] Fergeson JE, Patel SS, Lockey RF. Acute asthma, prognosis, and treatment. The Journal of Allergy and Clinical Immunology. 2017; 139: 438–447.

[6] Sharma R, Tiwari A, McGeachie MJ. Recent miRNA Research in Asthma. Current Allergy and Asthma Reports. 2022; 22: 231–258.

[7] Weidner J, Bartel S, Kılıç A, Zissler UM, Renz H, Schwarze J, *et al*. Spotlight on microRNAs in allergy and asthma. Allergy. 2021; 76: 1661–1678.

[8] Fan Q, Jian Y. MiR-203a-3p regulates TGF-β1-induced epithelial-mesenchymal transition (EMT) in asthma by regulating Smad3 pathway through SIX1. Bioscience Reports. 2020; 40: BSR20192645.

[9] Wang T, Zhou Q, Shang Y. MiRNA-451a inhibits airway remodeling by targeting Cadherin 11 in an allergic asthma model of neonatal mice. International Immunopharmacology. 2020; 83: 106440.

[10] Liu Y, Huo SG, Xu L, Che YY, Jiang SY, Zhu L, *et al*. MiR-135b Alleviates Airway Inflammation in Asthmatic Children and Experimental Mice with Asthma via Regulating CXCL12. Immunological Investigations. 2022; 51: 496–510.

[11] Li J, Zhu Y, Ma Z, Liu Y, Sun Z, Wu Y. miR-140 ameliorates neuropathic pain in CCI rats by targeting S1PR1. Journal of Receptor and Signal Transduction Research. 2021; 41: 401–407.

[12] Yin R, Jiang J, Deng H, Wang Z, Gu R, Wang F. miR-140-3p aggregates osteoporosis by targeting PTEN and activating PTEN/PI3K/AKT signaling pathway. Human Cell. 2020; 33: 569–581.

[13] Chiba Y, Ando Y, Fujii S, Miyakawa Y, Suto W, Kamei J, *et al*. Downregulation of miR-140-3p Is a Cause of Upregulation of RhoA Protein in Bronchial Smooth Muscle of Murine Experimental Asthma. American Journal of Respiratory Cell and Molecular Biology. 2021; 64: 138–140.

[14] Meng J, Zou Y, Hou L, He L, Liu Y, Cao M, *et al*. MiR-140-3p Ameliorates The Inflammatory Response of Airway Smooth Muscle Cells by Targeting HMGB1 to Regulate The JAK2/STAT3 Signaling Pathway. Cell Journal. 2022; 24: 673–680.

[15] Hu G, Du Y, Xie M, Chen R, Shi F. Circulating miRNAs act as potential biomarkers for asthma. Frontiers in Immunology. 2023; 14: 1296177.

[16] Yang W, Liu Y, Xu QQ, Xian YF, Lin ZX. Sulforaphene Ameliorates Neuroinflammation and Hyperphosphorylated Tau Protein via Regulating the PI3K/Akt/GSK-3β Pathway in Experimental Models of Alzheimer's Disease. Oxidative Medicine and Cellular Longevity. 2020; 2020: 4754195.

[17] Wang YM, Gong FC, Qi X, Zheng YJ, Zheng XT, Chen Y, *et al*. Mucin 1 Inhibits Ferroptosis and Sensitizes Vitamin E to Alleviate Sepsis-Induced Acute Lung Injury through GSK3β/Keap1-Nrf2-GPX4 Pathway. Oxidative Medicine and Cellular Longevity. 2022; 2022: 2405943.

[18] Zhang H, Ni M, Wang H, Zhang J, Jin D, Busuttil RW, *et al*. Gsk3β regulates the resolution of liver ischemia/reperfusion injury via MerTK. JCI Insight. 2023; 8: e151819.

[19] Huang X, Yu H, Xie C, Zhou YL, Chen MM, Shi HL, *et al*. Louki Zupa decoction attenuates the airway inflammation in acute asthma mice induced by ovalbumin through IL-33/ST2-NF-κB/GSK3β/mTOR signalling pathway. Pharmaceutical Biology. 2022; 60: 1520–1532.

[20] Yu Q, Yu X, Zhong X, Ma Y, Wu Y, Bian T, *et al*. Melatonin modulates airway smooth muscle cell phenotype by targeting the STAT3/Akt/GSK-3β pathway in experimental asthma. Cell and Tissue Research. 2020; 380: 129–142.

[21] Yin M, Chen W, Li M, Wang K, Hu N, Li Z. circAFF1 enhances intracerebral hemorrhage induced neuronal ferroptosis by targeting miR-140-5p to regulate GSK-3β mediated Wnt/β-catenin signal pathway. Brain Research Bulletin. 2022; 189: 11–21.

[22] Liu L, Li TM, Liu XR, Bai YP, Li J, Tang N, *et al*. MicroRNA-140 inhibits skeletal muscle glycolysis and atrophy in endotoxin-induced sepsis in mice via the WNT signaling pathway. American Journal of Physiology. Cell Physiology. 2019; 317: C189–C199.

[23] Nur Husna SM, Md Shukri N, Mohd Ashari NS, Wong KK. IL-4/IL-13 axis as therapeutic targets in allergic rhinitis and asthma. PeerJ. 2022; 10: e13444.

[24] Lodyga M, Hinz B. TGF-β1 - A truly transforming growth factor in fibrosis and immunity. Seminars in Cell & Developmental Biology. 2020; 101: 123–139.

[25] Aghasafari P, George U, Pidaparti R. A review of inflammatory mechanism in airway diseases. Inflammation Research: Official Journal of the European Histamine Research Society ... [et Al.]. 2019; 68: 59–74.

[26] Yao Z, Fu Y. Glycyrrhizic acid restrains airway inflammation

and remodeling in asthma via the TGF-β1/Smad signaling pathway. Experimental and Therapeutic Medicine. 2021; 21: 461.

[27] Ou G, Liu Q, Yu C, Chen X, Zhang W, Chen Y, *et al*. The Protective Effects of Maresin 1 in the OVA-Induced Asthma Mouse Model. Mediators of Inflammation. 2021; 2021: 4131420.

[28] Siddiqui S, Johansson K, Joo A, Bonser LR, Koh KD, Le Tonqueze O, *et al*. Epithelial miR-141 regulates IL-13-induced airway mucus production. JCI Insight. 2021; 6: e139019.

[29] Gu W, Li G, Zhang W, Zhang X, He Y, Huang L, *et al*. MiR-29b regulates Th2 cell differentiation in asthma by targeting inducible B7-H3 and STAT3. Clinical and Translational Allergy. 2022; 12: e12114.

[30] Ciprandi G, Tosca MA, Silvestri M, Ricciardolo FLM. Inflammatory biomarkers for asthma endotyping and consequent personalized therapy. Expert Review of Clinical Immunology. 2017; 13: 715–721.

[31] Vieira Braga FA, Kar G, Berg M, Carpaij OA, Polanski K, Simon LM, *et al*. A cellular census of human lungs identifies novel cell states in health and in asthma. Nature Medicine. 2019; 25: 1153–1163.

[32] Suárez-Cuartín G, Crespo A, Mateus E, Torrejón M, Giner J, Belda A, *et al*. Variability in Asthma Inflammatory Phenotype in Induced Sputum. Frequency and Causes. Archivos De Bronconeumologia. 2016; 52: 76–81.

[33] Zhang Y, Li B. Effects of montelukast sodium plus budesonide on lung function, inflammatory factors, and immune levels in elderly patients with asthma. Irish Journal of Medical Science. 2020; 189: 985–990.

[34] He XY, Simpson JL, Wang F. Inflammatory phenotypes in stable and acute childhood asthma. Paediatric Respiratory Reviews. 2011; 12: 165–169.

[35] Hao LY, Lu Y, Ma YC, Wei RP, Jia YP. MiR-140 protects against myocardial ischemia-reperfusion injury by regulating NF-κB pathway. European Review for Medical and Pharmacological Sciences. 2020; 24: 11266–11272.

[36] Samim Khan S, Janrao S, Srivastava S, Bala Singh S, Vora L, Kumar Khatri D. GSK-3β: An exuberating neuroinflammatory mediator in Parkinson's disease. Biochemical Pharmacology. 2023; 210: 115496.

[37] Duda P, Hajka D, Wójcicka O, Rakus D, Gizak A. GSK3β: A Master Player in Depressive Disorder Pathogenesis and Treatment Responsiveness. Cells. 2020; 9: 727.

[38] Jiang M, Zhang X, Yan X, Mizutani S, Kashiwazaki H, Ni J, *et al*. GSK3β is involved in promoting Alzheimer's disease pathologies following chronic systemic exposure to Porphyromonas gingivalis lipopolysaccharide in amyloid precursor protein$^{NL\text{-}F/NL\text{-}F}$ knock-in mice. Brain, Behavior, and Immunity. 2021; 98: 1–12.